

# EXPERIMENTAL ANALYSIS AND MODELING OF THE BUCKLING OF A LOADED HONEYCOMB SANDWICH COMPOSITE

## EKSPERIMENTALNA ANALIZA IN MODELIRANJE UPOGIBANJA OBREMENJENEGA SATASTEGA SENDVIČNEGA KOMPOZITA

**Abderrahmane Bentouhami, Boualem Keskes**

Laboratoire de mécanique de précision appliquée, Institut d'Optique et Mécanique de Précision, Université Ferhat Abbas de Sétif, Algérie  
bentouhamidahman@yahoo.fr, bkeskes2012@gmail.com

*Prejem rokopisa – received: 2014-02-22; sprejem za objavo – accepted for publication: 2014-03-28*

doi:10.17222/mit.2014.039

Sandwich panels have the best stiffness-to-lightness ratio, which is what makes them very useful in industrial applications. This paper is focused on a study of the buckling capacities of the core components under uniaxial compression. The critical buckling loads for various core densities and materials of honeycomb panels were experimentally and numerically investigated. The specimens under lateral loading showed three zones: zone 1 is the initial elastic state, followed by the plateau region in zone 2, while zone 3 shows a monotonically stiffening region, associated with the densification of the material. The effect of the core density and its materials on the behavior and the damage was highlighted. From the experiment it is clear that the buckling load of the specimens increases as the core density is increasing. In terms of stiffness and load at failure, the honeycomb sandwich panel had better mechanical characteristics than its components. The study also calculated the numerical buckling loads of the panels using the ABAQUS finite-element analysis program. The achieved experimental and numerical results were compared with each other. In conclusion, a good correlation between theory and experiment was found.

Keywords: honeycomb sandwich panel, buckling analysis, compression, finite-element method, collapse

Sendvični paneli imajo najboljše razmerje med togostjo in maso. To jih dela primerne za industrijsko uporabo. Ta članek je usmerjen v študij zdržljivosti za upogibanje ključnih komponent pri enoosni tlačni obremenitvi. Eksperimentalno in numerično so bile preiskane kritične upogibne obremenitve za različne ključne gostote in material satastih plošč. Vzorci, stransko obremenjeni, so pokazali tri področja: področje 1 je začetno elastično stanje, ki mu sledi področje platoja, tj. področje 2. Področje 3 prikazuje monotono upogibanje, povezano z zgoščevanjem materiala. Ocenjen je bil vpliv ključne gostote in materialov glede vedenja in poškodb. Iz preizkusov je razvidno, da z naraščanjem ključne gostote narašča tudi odpornost proti upogibni obremenitvi vzorcev. Glede na upogibanje in obremenitev pri porušitvi ima satasta sendvična plošča boljše mehanske lastnosti v primerjavi z njenimi komponentami. V študiji je tudi izračunana numerična upogibna obremenitev panelov z analizo končnih elementov s programom ABAQUS. Primerjani so dobljeni eksperimentalni in numerični rezultati. Dobljena je bila dobra korelacija med teorijo in eksperimentalnimi rezultati.

Ključne besede: satasta sendvična plošča, analiza upogibanja, tlačenje, metoda končnih elementov, porušitev

## 1 INTRODUCTION

Honeycomb sandwich panels are increasingly used in engineering applications (aviation, astronautics and navigation, automotive, etc.), where a high rigidity as well as lightness is important. A number of core materials and core configurations have been proposed recently. The most commonly used core materials are honeycombs and foams. Honeycomb sandwich panels are obtained by covering the upper and lower surfaces of the honeycomb with sheets. Metal or non-metal materials can be used as the lower and upper surface face sheet materials of honeycomb sandwich panels. The widespread use of honeycomb in practice generated a need to establish their mechanical properties. Previous studies on the crushing behavior of honeycomb structures included the early work reported by McFarland,<sup>1</sup> who developed a semi-empirical model to predict the crushing stress of hexagonal cell structures subjected to axial loading. This model as later improved to incor-

porate both the bending and extensional deformation of such cellular structures.<sup>2</sup>

Meanwhile, the mechanical properties of honeycomb structures in the lateral directions were investigated both analytically and experimentally by Gibson and Ashby,<sup>3</sup> and Gibson et al.<sup>4</sup> In their works, phenomenological models were proposed. More detailed analyses of the buckling of tubes with various geometries have been reported, and some of these results correlated well with the experimental data.<sup>5-9</sup> A more complete description of the buckling mechanisms for thin-walled tubular structures subjected to quasi-static and dynamic loading can be found in<sup>10,11</sup>. On the other hand, the mechanical behavior of sandwich composite panels made of honeycomb cellular structures has been studied extensively. For example, the force-indentation relationship for beams and plates made of sandwich polymer composites was investigated by Wu and Sun.<sup>12</sup> This relationship was later adopted by Lee and Tsotsis<sup>13</sup> to develop an impact model to predict the transient responses of sandwich composite

parcels. As for sandwich plates and shells whose faces were made of metal, experimental results have been reported by Goldsmith and Sackman.<sup>14</sup> A plasticity model has been reported by Jamjian et al.<sup>15</sup> for metallic sandwich panels subjected to impact, in which the honeycomb was treated as a continuum with a discontinuous density.

Kaman et al.<sup>16</sup> have experimentally and numerically investigated the behavior and failure mechanisms of honeycomb core panels. They have determined that the critical buckling load of Nomex is higher than that of aluminum comb composite panels for all cell sizes. Castanié et al.<sup>17</sup> showed that the compression load is essentially taken by the vertical edges of the hexagonal cell. From the axial compression collapse tests on the aluminum honeycomb sandwich panel specimen, various potential influential parameters, i.e., the core height, core-cell thickness and panel aspect ratio, it was observed that the core height would be a crucial parameter affecting the sandwich panel's ultimate compressive strength.<sup>18</sup> Tsang and Lagace<sup>19</sup> reported the different failure mechanisms in impact-damaged sandwich panels subjected to uniaxial compressive loads. They observed that the damage propagation and final failure modes were dependent on the relative extents of the core and face-sheet damage. They reported dimple propagation across the width of the panel, which occurred in the presence of core damage, with the final failure mode being a face-sheet fracture. Zhou and Mayer<sup>20</sup> studied the shear, tearing, and compression tests over honeycomb aluminum, which showed different failure modes involved in a general crash accident. Mohr and Do-yoyo,<sup>21,22</sup> Hong et al.<sup>23</sup> performed multi-axial loading tests of honeycomb materials and derived the macroscopic yield functions for the honeycomb materials. Wilbert et al.<sup>24</sup> proved that following an initial linear response, the cell walls buckle elastically. The post-buckling response is initially stiff and stable, but the inelastic action progressively softens it, leading to a limit load instability. The deformation localizes first at mid-height in the form of a sharp buckle, which with the load continuing to drop more into folding. When the walls of the fold come into contact, the local collapse is arrested, the load begins to recover, and a second fold develops on one side of the first one. The second fold in turn col-

lapses, forming a new load peak and a second trough. This progressive folding keeps repeating until the whole panel is consumed and the structure returns to a stiff response.

The present study is concerned with the more traditional problem of transverse compression. In particular, we aim to establish all aspects of the compressive response and explain the buckling phenomena of honeycomb sandwich structures. The critical buckling loads for various core densities and the materials of honeycomb panels are experimentally and numerically investigated. The different specimens exhibited similar load/displacement curves and the differences observed were only due to the behavior of the different materials. The study also calculates the numeric buckling loads of the panels using the ABAQUS finite-element analysis program. The achieved experimental and numerical results are compared with each other and the results are presented in curves. In conclusion, a good correlation between theory and experiment was found.

## 2 EXPERIMENTAL PROCEDURES

The critical buckling loads and crushing behavior of the honeycomb sandwich panels were determined by running through compression tests using a computerized universal testing machine Zwick/Roell (100 kN) (**Figure 1**). The test procedure for the compressive properties was

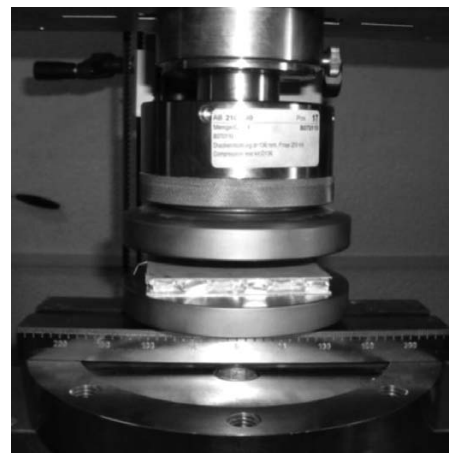


**Figure 1:** Experimental set-up of the compressive test  
**Slika 1:** Eksperimentalni sestav za tlačni preizkus

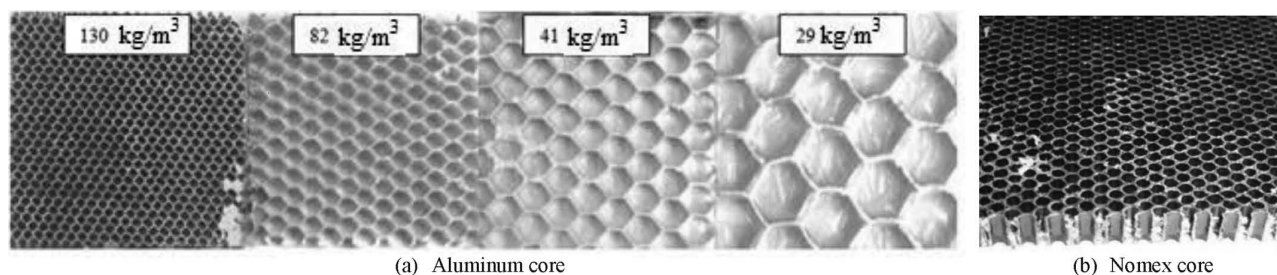


**Figure 2:** Typologies of investigated honeycomb sandwich: a) aluminum core, b) Nomex core  
**Slika 2:** Vrste preiskovanih satastih sendvičnih plošč: a) jedro iz aluminija, b) jedro nomex

as per the ASTM C 365 standards. Aluminum honeycomb with cell sizes of (3.2, 6.4, 9.6 and 19.2) mm and densities of (29, 41, 82 and 130) kg/m<sup>3</sup>, Nomex honeycomb with a cell size of 3.2 mm and densities of (48, 80, 128 and 144) kg/m<sup>3</sup> were used to complete the tests series (Figure 2). The dimension of the compressive specimen was 50 mm × 50 mm × 10 mm. The tests were performed at a constant cross-head speed of 0.5 mm/min.

2.1 Modeling of the cell walls of honeycomb composites

When the honeycomb composite was loaded in compressive mode, it was assumed that a uniform compression was achieved on the two edges parallel to the compressive loading direction of each wall, as shown in Figure 3. It was also assumed that the cell walls of the honeycomb composite were rigidly constrained by the neighboring cell walls and that all the cell walls were deformed to the same strain. Therefore, the compressive stress of the honeycomb composite is the sum of the stresses carried by the individual cell walls. The assumptions, due to its geometrical symmetry of the cross-section, are as follows:<sup>25</sup>

When the thickness  $h_c$  of a honeycomb core is not large compared with the length of side  $a$ , the buckling mode of a cell shell is based on a cell wall, every wall has a similar buckling mode, and the phases among the cell walls are the same or reversed. At the same time, every prismatic edge remains a straight line, and each cell wall looks like a rectangular thin-walled plate simply supported on all four edges.

If a sandwich panel with a hexagonal cell core is thick, the buckling mode of the cell shell is a deflection of the axial centerline, and the deformation of every prismatic edge is similar to that of the axial centerline. According to Equation (1), every wall becomes a rectangular, thin-walled, and simply supported on all four edges, as described in Figure 3. The buckling investigation on a cell wall can be substituted for that of the entire cell shell. The governing differential equation of the cell wall can be expressed as follows:

$$D \left( \frac{\partial^4 W}{\partial x^4} + 2 \frac{\partial^4 W}{\partial x^2 \partial y^2} + \frac{\partial^4 W}{\partial y^4} \right) + F_x \frac{\partial^2 W}{\partial x^2} \tag{1}$$

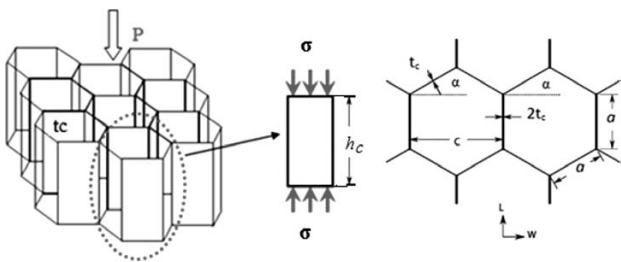


Figure 3: Modeling of honeycomb core with hexagonal cell under uniform compression loading

Slika 3: Modeliranje satastega jedra s heksagonalnimi celicami pri enakomerni tlačni obremenitvi

The boundary conditions are often written as:

$$W = 0, \frac{\partial^2 W}{\partial y^2} = 0 \text{ when } y = 0, a \tag{2}$$

$$W = 0, \frac{\partial^2 W}{\partial x^2} = 0 \text{ when } x = 0, h_c \tag{3}$$

Under the restriction of boundary conditions, the solution (local buckling) of Equation (1) can be written as:

$$W(x, y) = \sum_{m=1}^{\infty} \sum_{n=1}^{\infty} A_{mn} \sin \frac{m\pi x}{h_c} \sin \frac{n\pi y}{a} \tag{4}$$

The formula for a rectangular cell wall under equal uniform compression on two opposite edges,  $h_c$ , was shown as in Equation (5). The theoretical compressive stress on a cell wall used in this study was based on Zhang and Ashby's model and can be expressed as follows:

$$F = K_C \frac{E}{1-\nu^2} \left( \frac{t_c^3}{h_c} \right) \tag{5}$$

where  $K_C$  is the end constraint factor in the compression mode and its value<sup>26,27</sup> is 5.73,  $E$  is the elastic modulus of the cell walls,  $\nu$  is the Poisson's ratio of the cell walls,  $t_c$  is the thickness of the cell wall and  $h_c$  is the length of the free wall.

Equation (1) is expressed as the load  $F$  on a cell wall. The compressive load of the individual hexagonal cell of the honeycomb core is the sum of the loads carried by the individual cell walls. The total compressive load is  $10F$ , which is the sum of the compressive load,  $2F$ , carried out by the free walls with single thickness and the compressive load,  $8F$ , and carried by the ribbon with double thickness because the load is proportional to the cube of the thickness, as shown in Equation (5). The area,  $A_{hex}$ , of the individual hexagonal cell in a honeycomb core is calculated as  $2h_c \cos \alpha \times h_c \sin \alpha + 2h_c \cos \alpha \times h_c$ , where  $\alpha$  is the angle of the inclined cell wall. The compressive strength,  $\sigma_c$ , carried by the unit hexagonal cell, is expressed as in Equation (2):

$$\sigma_c = \frac{10F}{A_{hex}} = \frac{5K_C E}{(1-\nu^2) \cos(1+\sin \alpha)} \frac{t^3}{hc^3} \tag{6}$$

3 RESULTS AND DISCUSSION

Figure 4 shows a typical stress-strain curve obtained from a compressive test of the honeycomb composite.

The compressive deformation process can be categorized into three regions (1, 2 and 3) based on the compressive stress-strain behavior.

The figure shows that the stress-strain relationship is linear in Region 1 up to the bare compressive strength. The honeycomb cell walls are in the elastic buckling condition in Region 1 (Figure 5).

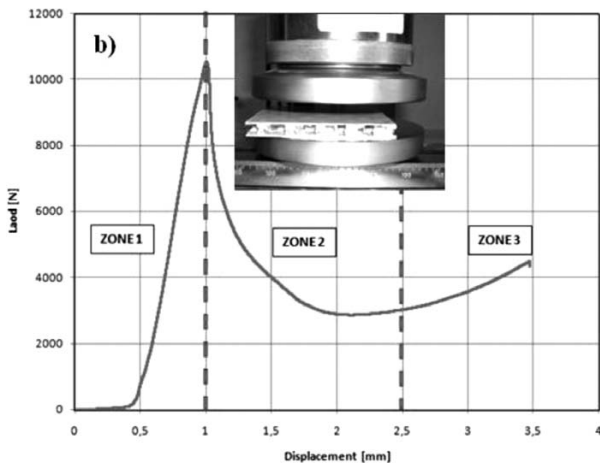


**Figure 4:** Load-displacement curve for an aluminum honeycomb sandwich

**Slika 4:** Krivulja obremenitev – raztezek satasto sendvične plošče iz aluminija

Later, a sudden decrease in the compressive stress occurs in Region 2. In this region, the core walls are in the plastic buckling condition and, as a result, wall folding occurs (**Figure 5**).

The compressive stress remains approximately stable in Region 3 until the densification of the folds in the honeycomb core. This stable stress value is defined as the crushing strength. In this region the crushing and fracture of the cores start (**Figure 5**). Depending on the core densification at the end of Region 3, an increase in the compressive stress is observed, as was reported in<sup>16-24</sup>.

Initial collapse occurs at a load that is about twice that of the average steady load causing progressive crushing. The amplitudes of the little peaks, which signify progressive folding collapse, are higher initially and gradually decrease, as shown in **Figure 4**. Plastic

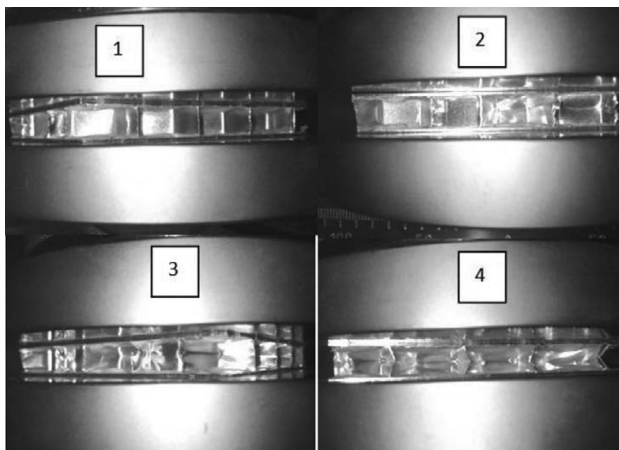


**Figure 5:** Stages of quasi-static compression test of aluminum honeycomb: (1) initial state, (2) buckling initiation, (3) progressive folding and (4) densification

**Slika 5:** Stopnje kvazistatičnega tlačnega preizkusa satja iz aluminija: (1) začetno stanje, (2) začetek upogibanja, (3) napredovanje zlaganja, (4) zgoščevanje

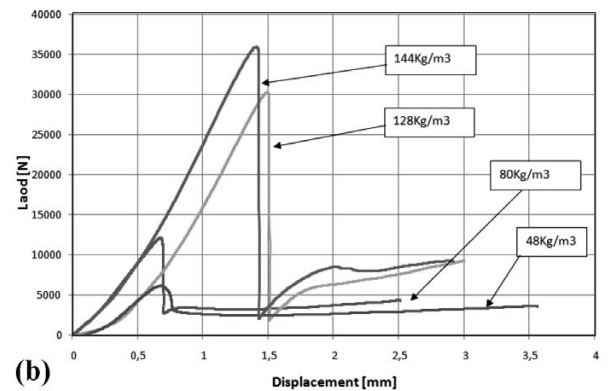
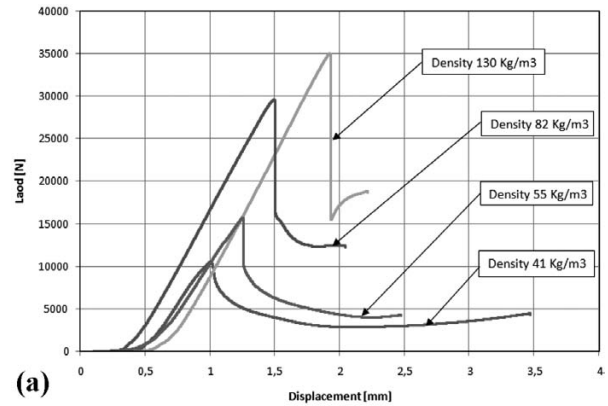


**Figure 6:** Load-displacement curves for honeycomb sandwich panels for different core densities: a) aluminum and b) Nomex

**Slika 6:** Krivulje obremenitev – raztezek za sataste sendvične panelne plošče z različno gostoto jedra: a) aluminij, b) nomex

collapse always occurred at one (usually the top) end and the deformation front gradually progressed with continued crushing until the plastic folding deformation approached the lower end of the specimen. Then the load increased very rapidly, indicating the densification of the specimen. The load-displacement graphics of the aluminum and Nomex honeycomb sandwich panels for different densities, resulting from the experiment, are given in

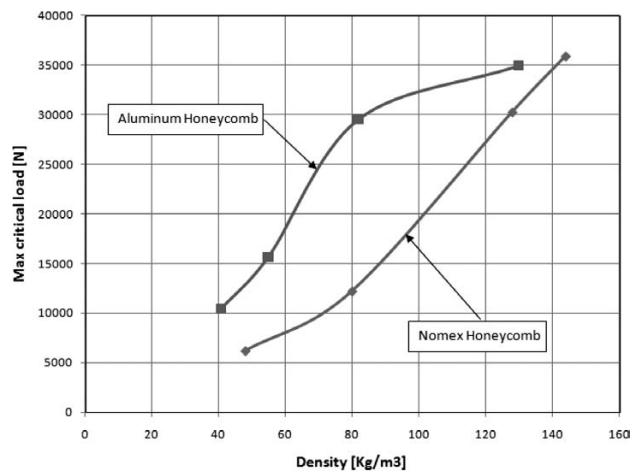


**Figure 7:** Evolution of the critical maximum load with the core density

**Slika 7:** Odvisnost kritične maksimalne obremenitve od gostote jedra

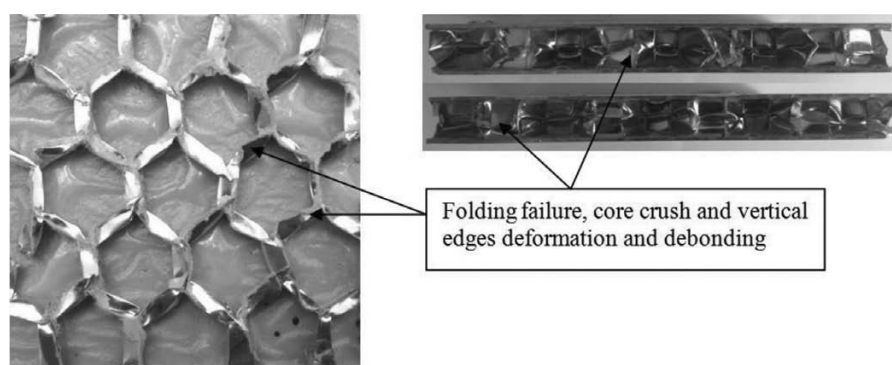


**Figure 8:** Failure mode of aluminum honeycomb sandwich  
**Slika 8:** Način porušitve satastega sendviča iz aluminija

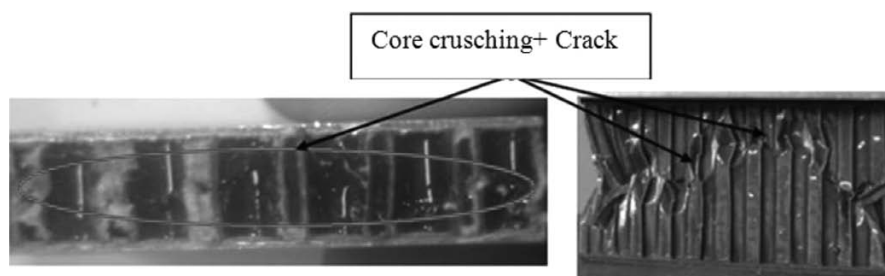


**Figure 9:** Failure modes of Nomex honeycomb panels for a cell size of 3.2 mm  
**Slika 9:** Način porušitve sataste plošče nomex z velikostjo celice 3,2 mm

**Figure 6.** It is clear that the maximum critical buckling load values of the aluminum core panels are higher than those of the Nomex core panels (**Figure 7**). Also, as the density increased, the compressive strength of both the Nomex and aluminum honeycomb panels increased.

The honeycomb compressive behavior intrinsically relates to the cell-wall buckling behavior under compression, because in reality the vertical cell walls can never be compressed along the length direction until a pure compressive failure due to the instability of the thin structure occurs. Therefore, the dominant mode of damage in these structures is the buckling of the cells' walls.

Besides the compressive strength, the establishment of the incurred failure modes during the experiment is also important. As the load increased, the initial honeycomb wall buckling and the later regional cell wall folding and core crushing were observed in the aluminum core sandwich panels (**Figure 8**). The failure modes of the Nomex panels under compression load show a similar behavior to that of the aluminum honeycomb. But for the Nomex core panels, which are more than aluminum, prior to the core crushing failure, crack generation occurred (**Figure 9**). The failure, which started as a cell-wall buckling, caused cracks under greater compression loads (**Figures 8 and 9**) than were reported in<sup>16,21–24</sup>. For the honeycomb core compressed in the axial direction, the localization occurs in the well-defined plastic collapse bands at the interface between the crushed and uncrushed structural regions.

**Figure 10** shows the evolution of the load for two different cell-wall thicknesses. From the obtained results, we see that the stiffness of the honeycomb sandwich panels increases with the cell-wall thickness.

To account for the influence of the thickness of the cell wall, the compression test has been made and the results of the variation of the load for two different wall thicknesses of the honeycomb core for a 6.4 mm cell size, the obtained results are given in the figure. According to the results of the experiment, we find that the wall thickness of the cell also has a significant impact on the

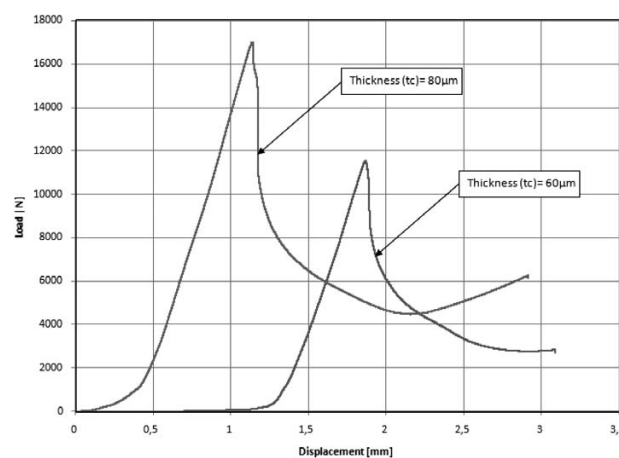


**Figure 10:** Effect of the cell-wall thickness on the buckling load for an aluminum honeycomb core

**Slika 10:** Vpliv debeline sten celic na obremenitev pri upogibu za satasto celico iz aluminija

critical buckling load. It is clear that the critical buckling load increased with an increase of the cell-wall thickness.

#### 4 NUMERICAL STUDY

The ABAQUS package program, based on the finite-element method, is used as the solution method to numerically establish the critical buckling loads and the complex compressive response and crushing of honeycomb sandwich panels after the buckling observed in the experiments. The shell elements are appropriate because the thickness is the smallest planar dimension (Figures 11 and 12). The finite-element mesh uses the fully integrated S4R shell element as a regular mesh with nearly square elements, while the number of elements used was selected from convergence studies. The panels, for which the compression test was performed, are three-dimensional and the mechanical properties of the utilized materials are given in Table 1.

**Table 1:** Sizes cell and mechanical properties of used core materials for modeling

**Tabela 1:** Velikost celic in mehanske lastnosti uporabljenih materialov za jedra za modeliranje

Density (kg/cm <sup>3</sup> )	$h_c$ /mm	$S$ /mm	$t_c$ /mm	$E_c$ /MPa	$\nu_c$
29	8.8	19.2	0.080	69000	0.3

To study the sensitivity of the critical buckling load with various parameters, such as the cell's number, the cell's size and the thickness of the cell wall, we con-

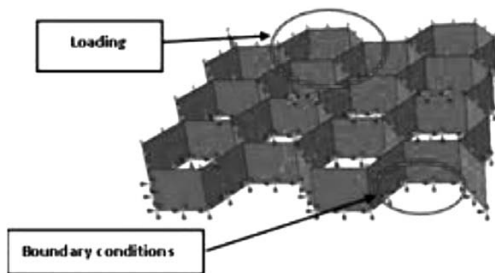


**Figure 11:** Finite-element model and boundary conditions of honeycomb sandwich panels

**Slika 11:** Model končnih elementov in robni pogoji za satasto sendvično ploščo

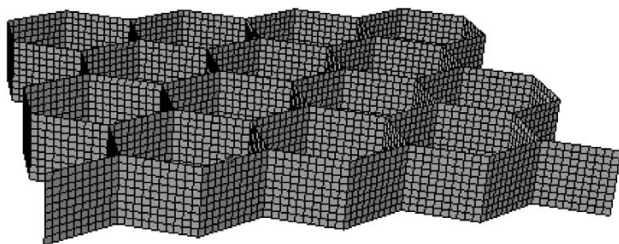


**Figure 12:** Finite-element mesh (S4R) model for buckling simulation of honeycomb sandwich panel

**Slika 12:** Model mreže končnih elementov (S4R) za simulacijo upogibanja sataste sendvične plošče

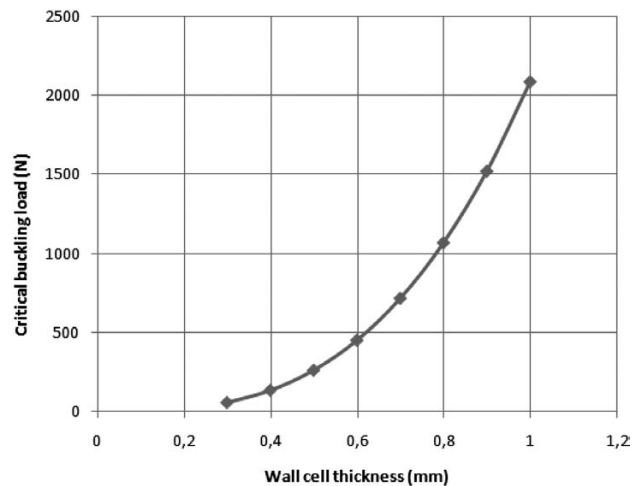


**Figure 13:** Variation of buckling load with cell-wall thickness for different honeycomb core materials for a cell size 19.2 mm

**Slika 13:** Spreminjanje obremenitve pri upogibanju v odvisnosti od debeline stene celice za različne materiale satastega jedra pri velikosti celice 19,2 mm

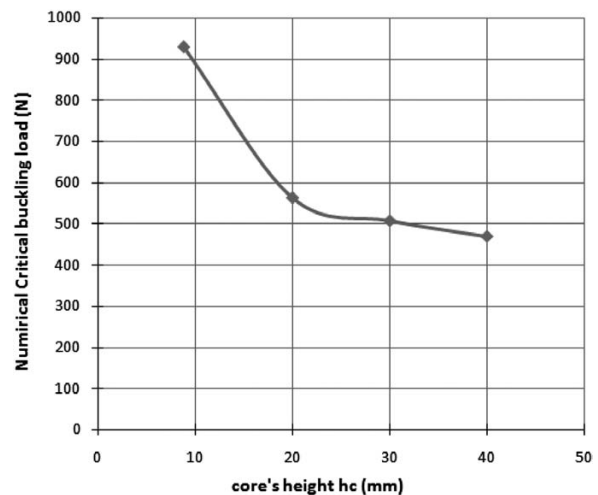


**Figure 14:** Variation of the numerical critical buckling load ( $F_{cn}$ ) with the core thickness ( $h_c$ )

**Slika 14:** Spreminjanje numerične kritične obremenitve ( $F_{cn}$ ) pri upogibu z debelino jedra ( $h_c$ )

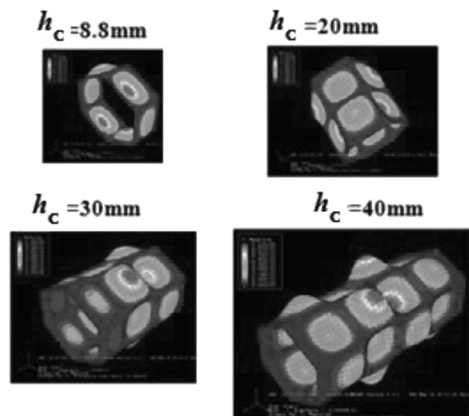


**Figure 15:** Buckling shapes for different values of  $h_c$

**Slika 15:** Oblike upogibanja pri različnih vrednostih  $h_c$

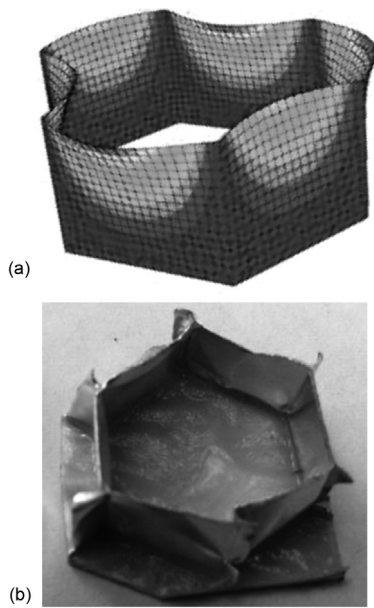


**Figure 16:** a) Experimental and b) numerical deformation of aluminum honeycomb for a cell size of 19.2 mm

**Slika 16:** a) Eksperimentalna in b) numerična deformacija satja iz aluminija za velikost celice 19,2 mm

ducted the following simulation runs on the finite-element code ABAQUS.

To account for the influence of the cell-wall thickness, simulations using the finite element code were made and the results of the variation of the numerical critical buckling load and the cell-wall thickness of the honeycomb sandwich panels for 19.2 mm cell sizes obtained are given in **Figure 13**. According to the results of the simulation, we find that the wall thicknesses of the cell have a significant impact on the critical buckling load and the resistance of the honeycomb sandwich panels. It is established that the critical buckling load increased with an increase of the cell-wall thickness.

To explain the effect of the core's thickness ( $h_c$ ) on the numerical critical buckling ( $F_{cn}$ ), the differences applications on the finite-elements code ABAQUS are realized. We can simply understand from **Figure 14** that by increasing the height of the core ( $h_c$ ), the value of the numerical critical buckling load ( $F_{cn}$ ) decreases.

The different values of ( $h_c$ ), ( $F_{cn}$ ) and the corresponding analytical buckling equations are summarized in **Table 2**. The buckling modes obtained for each ( $h_c$ ) are shown in **Figure 15**. **Figure 16** represents a comparison between failure modes of one cell obtained from experiment and numerical results for aluminum honeycomb core with cell's size of 19.2 mm.

**Figure 17** shows the evolution of the critical buckling load with the cell number of the honeycomb core for a 19.2 mm cell size. From the obtained results it is clear that the stiffness of the honeycomb sandwich panels increases with the number of cells. It is seen that the experimental and numerical deformation conditions are relatively coherent.

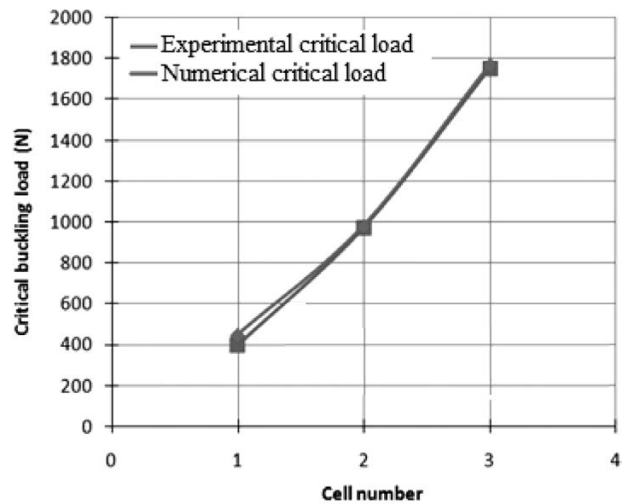


**Figure 17:** Variation of buckling load with the cell number for honeycomb core materials for a 19.2 mm cell size

**Slika 17:** Spreminjanje upogibne obremenitve s številom celic za material s satastim jedrom pri velikosti celice 19,2 mm

**Table 2:** Different height of core ( $h_c$ ) with correspondent buckling load ( $F_{cn}$ ) and analytical equations of buckling

**Tabela 2:** Različne višine jeder ( $h_c$ ) s pripadajočo obremenitvijo pri upogibu ( $F_{cn}$ ) in analitsko enačbo upogibanja

$h_c$	$R = h_c/a$	$F_{cn}/N$	analytical equations of buckling
8.8	$\sqrt{2} \geq R$	928.8	$W(x,y) = A_{11} \sin \frac{\pi x}{h_c} \sin \frac{\pi y}{a}$
20	$\sqrt{2} \leq R \leq \sqrt{6}$	562.67	$W(x,y) = A_{21} \sin \frac{2\pi x}{h_c} \sin \frac{\pi y}{a}$
30	$\sqrt{6} \leq R \leq \sqrt{12}$	507	$W(x,y) = A_{31} \sin \frac{3\pi x}{h_c} \sin \frac{\pi y}{a}$
40	$\sqrt{12} \leq R \leq 2\sqrt{5}$	469	$W(x,y) = A_{41} \sin \frac{4\pi x}{h_c} \sin \frac{\pi y}{a}$

## 5 CONCLUSIONS

The buckling load of sandwich plates with a honeycomb core subjected to compression damage has been investigated experimentally and numerically. The cell size and the wall thickness, and the materials, are parameters that have to be determined with respect to the usage area of the honeycomb sandwich structures optimally. The honeycomb compressive behavior intrinsically relates to the cell-wall buckling behavior under in-plane compression, because in reality the vertical cell walls can never be compressed along the length direction until a pure compressive failure due to the instability of the thin structure occurs. The following are the obtained results of the study:

- The critical buckling load of aluminum panels is determined to be higher than that of the Nomex honeycomb panels.
- The failure modes of the Nomex honeycomb sandwich panels under compression load show similar

behavior as that of the aluminum honeycombs. However, for the Nomex core panels, which are much more brittle than aluminum, prior to the core crushing failure, crack generation incurred.

- As the core's density increased, the maximum critical buckling load increased, both for the Nomex and the aluminum comb panels.
- It was observed that the core's height is a crucial parameter affecting the ultimate compressive strength of the sandwich panel.
- Besides the core's densities and the core height, the core-wall thickness also has an important effect on the critical buckling load. The critical buckling load increased as the cell-wall thickness increased.

## 6 REFERENCES

- <sup>1</sup> R. K. McFarland Jr, Hexagonal cell structures under post-buckling axial load, *AIAA Journal*, 1 (1963) 6, 1380–1385, doi:10.2514/3.1798
- <sup>2</sup> T. Wierzbicki, Crushing analysis of metal honeycombs, *International Journal of Impact Engineering*, 1 (1983) 2, 157–174, doi:10.1016/0734-743X(83)90004-0
- <sup>3</sup> L. J. Gibson, M. F. Ashby, *Cellular Solids, Structure and Properties*, Pergamon Press, Oxford 1988
- <sup>4</sup> L. J. Gibson, M. F. Ashby, G. S. Schajer, C. I. Robertson, The mechanics of twodimensional cellular materials, *Proc. R. Soc. Lond. A*, 382 (1982), 43–59, doi:10.1098/rspa.1982.0087
- <sup>5</sup> D. Mohr, T. Wierzbicki, Crushing of soft-core sandwich profiles: experiments and analysis, *International Journal of Mechanical Sciences*, 45 (2003) 2, 253–271, doi:10.1016/S0020-7403(03)00053-5
- <sup>6</sup> W. Abramowicz, T. Wierzbicki, Axial crushing of multicorner sheet metal columns, *Journal of Applied Mechanics*, 56 (1989) 1, 113–120, doi:10.1115/1.3176030
- <sup>7</sup> S. Li, S. R. Reid, Relationship between the elastic buckling of square tubes and rectangular plates, *Journal of Applied Mechanics*, 57 (1990) 4, 969–973, doi:10.1115/1.2897669
- <sup>8</sup> W. Abramowicz, N. Jones, Dynamic axial crushing of square tubes, *International Journal of Impact Engineering*, 2 (1984) 2, 179–208, doi:10.1016/0734-743X(84)90005-8
- <sup>9</sup> W. Abramowicz, N. Jones, Dynamic axial crushing of circular tubes, *International Journal of Impact Engineering*, 2 (1984) 3, 263–281, doi:10.1016/0734-743X(84)90010-1
- <sup>10</sup> N. Jones, *Structural Impact*, Cambridge University Press, Cambridge 1989
- <sup>11</sup> W. Johnson, S. R. Reid, Metallic energy dissipating systems, and the update, *Applied Mechanics Reviews*, 31 (1978), 277–288, Updated in: 39 (1986), 315-319
- <sup>12</sup> C. L. Wu, C. T. Sun, Low velocity impact damage in composite sandwich beams, *Composite Structures*, 34 (1996) 1, 21-27, doi:10.1016/0263-8223(95)00127-1
- <sup>13</sup> S. M. Lee, T. K. Tsotsis, Indentation failure behaviour of honeycomb sandwich panels, *Composites Science and Technology*, 60 (2000) 8, 1147–1159, doi:10.106/S0266-3538(00)00023-3
- <sup>14</sup> W. Goldsmith, J. L. Sackman, An experimental study of energy absorption in impact on sandwich plates, *International Journal of Impact Engineering*, 12 (1992) 2, 241–262, doi:10.1016/0734-743X(92)90447-2
- <sup>15</sup> M. Jamjian, J. L. Sackman, W. Goldsmith, Response of an infinite plate on a honeycomb foundation to a rigid cylindrical impactor, *International Journal of Impact Engineering*, 15 (1994) 3, 183–200, doi:10.1016/S 0734-743X(05)80012-0
- <sup>16</sup> M. O. Kaman, M. Y. Solmaz, K. Turan, Experimental and Numerical analysis of Critical Buckling Load of Honeycomb Sandwich panels, *Journal of Composite Materials*, 44 (2010) 24, 2819-2831, doi:10.1177/0021998310371541
- <sup>17</sup> B. Castanić, C. Bouvet, Y. Aminanda, J. J. Barrau, P. Thevenet, Modelling of low-energy/low-velocity impact on Nomex honeycomb sandwich structures with metallic skins, *International Journal of Impact Engineering*, 35 (2008) 7, 620–634, doi:10.1016/j.ijimpeng.2007.02.008
- <sup>18</sup> M. Giglio, A. Manes, A. Gilioli, Investigations on sandwich core properties through an experimental – numerical approach, *Composites: Part B: Engineering*, 43 (2012) 2, 361–374, doi:10.1016/j.compositesb.2011.08.016
- <sup>19</sup> P. H. W. Tsang, P. A. Lagace, Failure Mechanisms of Impact-damaged Sandwich Panels Under Axial Compression, *AIAA*, (1994) 1396, 745–754, doi:10.2514/6.1994-1396
- <sup>20</sup> Q. Zhou, R. R. Mayer, Characterization of Aluminum Honeycomb Material Failure in Large Deformation Compression, Shear and Tearing, *Journal of Engineering Materials and Technology*, 124 (2002) 4, 412-420, doi:10.1115/1.1491575
- <sup>21</sup> D. Mohr, M. Doyoyo, Large plastic deformation of metallic honeycomb: orthotropic rate-independent constitutive model, *International Journal of Solids and Structures*, 41 (2004) 16-17, 4435–4456, doi:10.1016/j.ijsolstr.2004.02.062
- <sup>22</sup> D. Mohr, M. Doyoyo, Deformation-induced folding systems in thin-walled monolithic hexagonal metallic honeycomb, *Int. J. Solids Struct.*, 41 (2004) 41, 3353–3377, doi:10.1016/j.ijsolstr.2004.01.014
- <sup>23</sup> S. T. Hong, J. Pan, T. Tyan, P. Prasad, Quasi-static Crush Behaviors of Aluminum Honeycomb Specimens under Compression Dominant Combined Loads, *International Journal of Plasticity*, 22 (2006) 1, 73–109, doi:10.1016/j.ijplas.2005.02.002
- <sup>24</sup> A. Wilbert, W. J. Jang, S. Kyriakides, J. F. Floccari, Buckling and progressive crushing of laterally loaded honeycomb, *International Journal of Solids and Structures*, 48 (2011) 5, 803–816, doi:10.1016/j.ijsolstr.2010.11.014
- <sup>25</sup> S. Liang, H. L. Chen, Investigation on the square cell honeycomb structures under axial loading, *Composite Structures*, 72 (2006) 4, 446–454, doi:10.1016/j.compstruct.2005.01.022
- <sup>26</sup> H. S. Lee, S. H. Hong, J. R. Lee, Y. K. Kim, Mechanical behavior and failure process during compressive and shear deformation of honeycomb composite at elevated temperatures, *Journal of Materials Science*, 37 (2002) 6, 1265-1272, doi:10.1023/A:1014344228141
- <sup>27</sup> X. Fan, I. Verpoest, D. Vandepitte, Finite Element Analysis of Out-of-plane Compressive Properties of Thermoplastic Honeycomb, *Journal of Sandwich Structures and Materials*, 8 (2006) 5, 437-458, doi:10.1177/1099636206065862